

⁷B. D. Martin and C. V. Heer, *Phys. Rev.* **173**, 631 (1968).

⁸J. Itoh, Y. Masuda, K. Asayama, and S. Kobayashi, *J. Phys. Soc. Japan* **18**, 455 (1963).

⁹O. Nagai, *J. Phys. Soc. Japan* **20**, 2300 (1965).

¹⁰C. W. Kimball, W. C. Phillips, M. V. Nevitt, and R. S. Preston, *Phys. Rev.* **146**, 375 (1966).

¹¹V. Jaccarino and J. A. Seitchik, *Bull. Am. Phys. Soc.* **10**, 317 (1956).

¹²J. A. Seitchik, V. Jaccarino, and J. H. Wernick, *Bull. Am. Phys. Soc.* **10**, 317 (1965).

¹³C. P. Gazzara, R. M. Middleton, R. J. Weiss, and E. O. Hall, *Acta Cryst.* **22**, 859 (1967).

¹⁴J. A. Oberteuffer and J. A. Ibers, *Acta Cryst.* (to be published).

¹⁵J. A. Oberteuffer and J. A. Marcus, *Bull. Am. Phys. Soc.* **13**, 58 (1968).

¹⁶L. H. Schwartz, *Nucl. Instr. Methods* **42**, 81 (1966).

¹⁷A local version of a general least-squares refinement program useful for overlapping reflections.

¹⁸A local version of ORFLS, a least-squares refinement program described in ORNL Report No. TM-305 (unpublished).

¹⁹J. M. Hastings, N. Elliot, and L. M. Corliss, *Phys. Rev.* **115**, 13 (1959).

²⁰Magnetic-torsion-balance measurements made by one of us (J. A. O.) also indicate that the magnetic point group is tetragonal. These measurements [Ref. 15 and J. A. Oberteuffer, Ph.D. thesis, Northwestern University, 1969 (unpublished)] of the temperature and magnetic field dependence of the twofold and fourfold torques about 100 crystallographic axes below T_N show an anomalous behavior in the fourfold torque.

²¹R. E. Watson and A. J. Freeman, *Acta Cryst.* **14**, 231 (1961).

²²T. Yamada, *J. Phys. Soc. Japan* **28**, 596 (1970);

T. Yamada and S. Tazawa, *ibid.* **28**, 609 (1970); T. Yamada, N. Kunitomi, Y. Nakai, D. E. Cox, and G. Shirane, *ibid.* **28**, 615 (1970).

Dielectric Properties of Strontium Titanate at Low Temperature

M. A. Saifi* and L. E. Cross

Materials Research Laboratory and Department of Electrical Engineering,

The Pennsylvania State University, University Park, Pennsylvania 16802

(Received 5 February 1968; revised manuscript received 21 January 1970)

The dielectric properties of annealed single crystals of SrTiO_3 have been measured over the temperature range from 5 to 300 °K. At temperatures below 50 °K, electric double hysteresis loops are observed and associated changes in weak-field permittivity under dc bias have been measured. It is shown that a phenomenological analysis based on the simple Kittel function accounts satisfactorily for many aspects of the dielectric behavior of SrTiO_3 crystals.

I. INTRODUCTION

Strontium titanate is of considerable interest as a low-temperature perovskite ferroelectric. The Cochran ferroelectric mode was first observed in this material by infrared^{1,2} and by neutron spectrometry.³ It is well known that a phase transition occurs at about 110 °K, which involves a symmetry change from pseudocubic to tetragonal and is evidenced by the rapid onset of twinning.⁴⁻⁶ Further evidence is obtained through electron-paramagnetic-resonance^{7,8} (EPR) measurements of Fe- and Gd-doped SrTiO_3 . There is no apparent discontinuity in the dielectric constant⁹⁻¹¹ or its slope at this temperature. Recent measurements by Fleury, Scott, and Worlock¹² and by Shirane and Yamada¹³ have shown that the phase change is associated with a "crumpling" of the regular array of oxygen octahedra, in which the individual octahedron rotates about a fourfold axis.

The dielectric constant of SrTiO_3 follows a Curie-Weiss law with a Curie temperature of 40 °K. Weaver⁹ observed weak hysteresis below 62 °K and concluded that SrTiO_3 goes through a second-order phase transition to a ferroelectric state.

In this paper we present evidence for a possible antiferroelectric phase transition at about 62 °K in carefully annealed single-crystal SrTiO_3 .

II. ANNEALING

The procedure used was in many respects similar to that used earlier by Paladino *et al.*¹⁴ Annealing was carried out in a special high-temperature Centorr electric (tungsten) furnace, which was modified for continuous operation with the sample in normal air atmosphere at 1900 °C. The annealing procedure consisted of heating to 1850 °C, maintaining this temperature for 6 h, slow cooling at the rate of 100 °C/h to 1300 °C, then shutting off

and allowing the sample to come to room temperature in about 6 h.

The results of the annealing were checked by optical and etch pit techniques. In the unannealed crystal, strain birefringence patterns similar to those reported by Lytle⁵ and by Cross and Chakravorty⁶ were observed. The annealed crystal remained dark under crossed polars, and the required compensation was below the limit of resolution of our equipment ($\pm 1^\circ$ with a Brace-Kohler $\frac{1}{8}\lambda$ compensator). Assuming uniform strain and applying the Giardini¹⁵ values of the stress optic coefficients, the c/a ratio in the annealed plate is less than 1.000 0012. This may be compared with the c/a ratio of order 1.000 08 reported by Lytle⁵ and of order 1.000 05 in the unannealed crystals reported by Cross and Chakravorty.⁸

The dislocations were revealed by etching the crystals in an etchant of five parts HF, ten parts HNO₃, and ten parts H₂O. Rhodes¹⁶ has shown that this etchant produces dislocation etch pits. Typical etch pit counts were $1.5 \times 10^6 \text{ cm}^{-2}$ in the unannealed crystal and $3 \times 10^5 \text{ cm}^{-2}$ in the annealed crystal. In general, annealing reduced the dislocation density by a factor of 3–7. The impurity content of the crystal was checked by the comparative spectrochemical analysis, and no difference was found before and after annealing. A typical result of the spectrochemical analysis is presented in Table I.

Finally, the 110 °K phase-transition temperature was carefully checked and was found to be (110 ± 1) °K for both the annealed and the unannealed crystal. The twin configuration in the annealed crystal was of about the same complexity as in the unannealed crystals.

III. DIELECTRIC PROPERTIES

A. Experimental Technique

Gold electrodes extending to the crystal edges

TABLE I. Impurity content of strontium titanate supplied by the National Lead Co., N. J.

Element	Level (ppm)
Si	200
Fe	< 10
Al	< 20
Sb	< 100
Sn	< 200
Mg	1–10
Cu	10–50
Pb	< 100
Mn	< 10
Ni	< 50
V	< 20
Cr	< 50
Zr	< 20

were vacuum evaporated on the major faces of thin crystal plates of approximate size $4 \times 4 \times 0.4$ mm. The samples were mounted in a Superior Air Co. helium cryostat, and capacitance was measured by a three-terminal method using a GR 1615A capacitance bridge at 1 kHz with a field level of $< 2 \text{ V/cm}$. The samples were kept in complete darkness during the measurements which were carried out over the slow natural rise in the temperature of the cryostat, after it had been cooled to helium temperature.

B. Unannealed Crystals

Measurements on unannealed crystals gave weak-field permittivities in qualitative agreement with earlier data. Typical curves for measurements with the field applied along the [100] direction are shown in Fig. 1. Similar data were taken for the [110] and [111] directions.

As with earlier studies, the permittivity from room temperature to 100 °K follows very closely a modified Curie-Weiss law:

$$\epsilon = 40 + (8.5 \times 10^4)/(T - 40) .$$

Below 90 °K the dielectric constant begins to deviate from the Curie-Weiss law, but no dielectric anomaly is observed at 40 °K. Weak anisotropy develops near 70 °K and becomes more pronounced at still lower temperatures. A particular feature of these data which appears to occur in all previous measurements, but is perhaps not sufficiently stressed, is that the virgin crystal gives the highest weak-field dielectric constant, which is irreversibly lowered after the application of an electric field. Under high fields the dielectric constant shows a broad maximum in its temperature dependence and the temperature at which this maximum occurs shifts toward higher values with increasing fields.

C. Dielectric Properties of Annealed Crystal in [100] Orientation

Above 62 °K, the weak-field dielectric behavior is similar to that of an unannealed crystal. Below this temperature, the dielectric constant exhibits quite different characteristics, depending upon whether the sample is cooled with the electrodes open circuited or short circuited. If cooled short circuited, the permittivity is much lower and is reproducibly given by curve K_A in Fig. 2. When cooled open circuited, the dielectric constant is higher and may show a range of values on different cooling runs; two typical curves are shown in Fig. 2 [(a) and (b)]. The highest dielectric constant measured in this state (see curve x in Fig. 2) was 24 600 at 5 °K, which is similar to that of an unannealed sample.

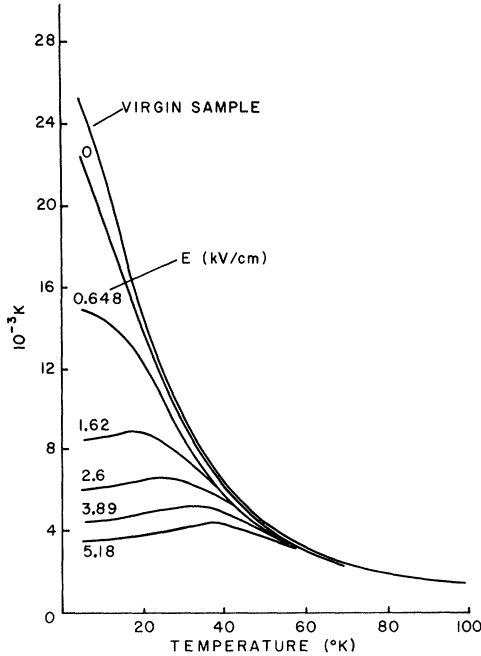


FIG. 1. Temperature dependence of weak-field dielectric permittivity for an unannealed crystal of SrTiO_3 with measuring field in [100] direction and dc bias fields along [100].

In the low permittivity state the crystal exhibits double hysteresis in its P - E relationship. The observed loops, obtained through a standard Sawyer and Tower circuit, at 60 Hz, for the temperature range of 5–38 °K are given in Fig. 3. The critical field at which a discontinuity in P is observed increases with temperature. The critical-field values as a function of temperature are shown by small circles in Fig. 4.

The double hysteresis was further confirmed by measuring the weak-field permittivity as a function of dc biasing fields. The results of such measurements at 5 °K are given in Fig. 5. In this figure the field-dependent behavior of the same crystal in its high permittivity state is also depicted.

IV. DISCUSSION

A. Phenomenological Analysis of Unannealed Crystal

Below 110 °K, SrTiO_3 is not strictly cubic, but as Cross and Chakravorty⁶ and Lytle⁵ have shown, even at very low temperatures the deviations from cubic symmetry are small. To some extent this is also borne out by the present dielectric measurements in the three orientations [100], [110], and [111]. It is not implied that the dielectric constant is truly isotropic, but that the anisotropy, espe-

cially under high fields, is small enough to treat the crystal as of cubic symmetry.

In this approximation the full Gibbs function for zero stress is given by

$$G = G_0 + f(T)(P_x^2 + P_y^2 + P_z^2) + B(P_x^4 + P_y^4 + P_z^4) + C(P_x^2 P_y^2 + P_y^2 P_z^2 + P_z^2 P_x^2) - \vec{E} \cdot \vec{P}, \quad (1)$$

wherein the higher-order polarization terms have been neglected and $2f(T)$ represents the temperature-dependent weak-field reciprocal susceptibility.

Following a procedure similar to that of Hegenbarth,¹⁰ but without using an explicit function for $f(T)$, the following relations can be derived:

$$\begin{aligned} (\bar{\chi}_{100})^{3/2} &= (54B)^{1/2} E_{100}, \\ (\bar{\chi}_{110})^{3/2} &= (54B + 27C)^{1/2} E_{110}/\sqrt{2}, \\ (\bar{\chi}_{111})^{3/2} &= (54B + 54C)^{1/2} E_{111}/\sqrt{3}, \end{aligned} \quad (2)$$

where $\bar{\chi}$ represents the minimum value of $\chi(E, T)$ for a fixed-field value.

The slopes of $\bar{\chi}^{3/2}$ -versus- E lines yield B and C coefficients. The data in the [100] and [110] orientations give $B = 0.135 \times 10^{10}$ and $C = 0.210 \times 10^{10}$, whereas from the slopes of [100]- and [111]-orientation data $C = 0.245 \times 10^{10}$, the units being $\text{V}^5 \text{m}^{-5} \text{C}^3$. The fair agreement in the values of coefficient C obtained from two independent measurements suggests that the assumption of cubic symmetry is a reasonable approximation.

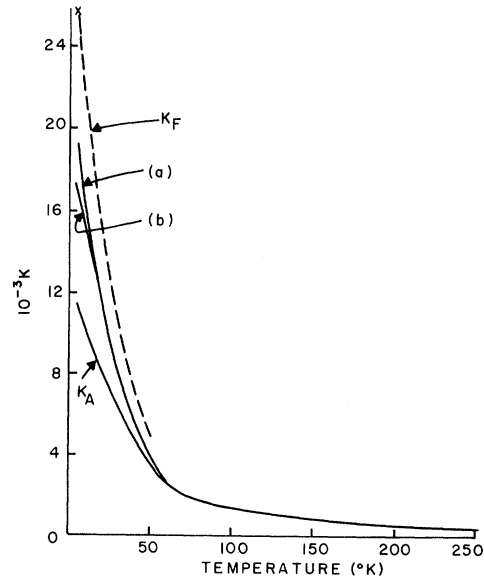
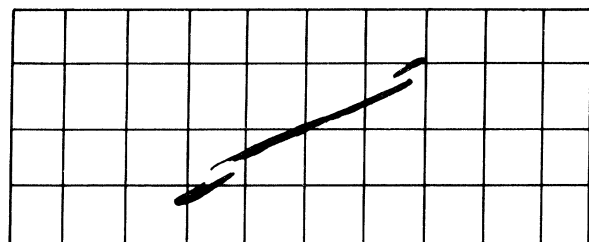
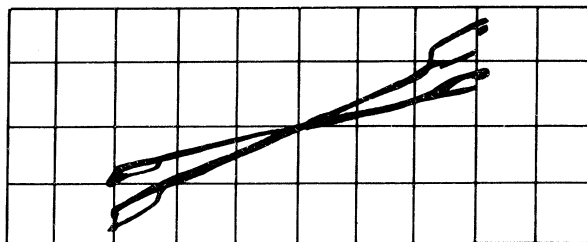


FIG. 2. Temperature dependence of weak-field dielectric permittivity for an annealed crystal of SrTiO_3 with measuring field in [100] direction. K_A : antiferroelectric state; K_F : paraelectric state, from an unannealed crystal; (a) and (b): mixed states; x: refer to the text.



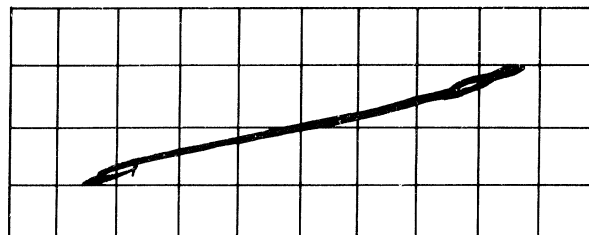
(a) 5°K



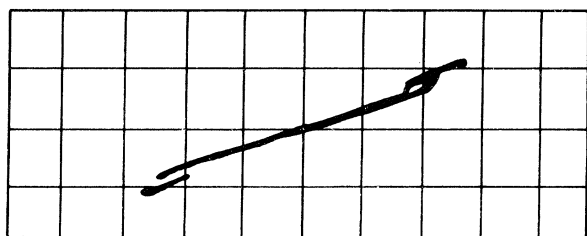
(d) 25°K



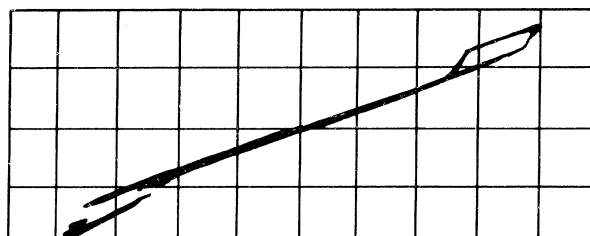
(b) 11°K



(e) 32°K



(c) 19°K



(f) 38°K

FIG. 3. Electric double hysteresis loops at several temperatures in an annealed crystal of SrTiO_3 . Crystal thickness is 0.045 cm; crystal area is 0.0684 cm^2 . Abscissa applied volts, one major division 18 V for (a) - (d) and 21.5 V for (e) and (f). Ordinate polarization, one major division 0.1 V for (a)-(e) and 0.05 V for (f) and the upper trace of (d). Integrating capacitor 0.911 μF .

Calculating the dielectric stiffness directly from the second partial derivative of the energy function, with these values of coefficients, gives curves for the three orientations [100], [110], and [111] over the range 5-40 °K, which agree within $\pm 10\%$ with the measured values.

The value of B obtained above is in reasonable accord with values given by Hegenbarth¹⁰ and

Itschner¹¹ from dielectric measurements. From electric-field-induced Raman scattering, Fleury and Worlock¹⁷ have also determined these coefficients. They find B to be temperature dependent, and considerably larger, and give for C a value 0.75×10^{10} . The electric field dependence of χ calculated from these values is considerably greater than observed in our dielectric measurements.

B. Phenomenological Analysis for Annealed Crystal

In annealed crystals we assume that on cooling under short-circuit conditions the crystal in its lowest-energy state for all temperatures below 62 °K is antiferroelectric. The very close similarity in behavior between annealed crystals cooled open circuited, unannealed crystals, and short-circuited crystals on the arms of the double loop, suggests strongly that the switching is from antiferroelectric to a field polarized paraelectric state.

Phenomenological analysis for this case can be carried out using the simple Kittel free-energy function

$$G = G_0 + f(P_a^2 + P_b^2) + gP_aP_b + h(P_a^4 + P_b^4) - E(P_a + P_b) \quad (3)$$

For antiferroelectric-ferroelectric switching, the phenomenology has been developed by Cross¹⁸; for antiferroelectric-paraelectric switching Okada¹⁹ has very recently completed the development. Unfortunately, the normalization procedure used in the last paper is not very suitable for our purpose, so we develop the required relations here. A more convenient form for the Kittel function is that due to Devonshire,²⁰ in which

$$G = G_0 + \frac{1}{2}(f + \frac{1}{2}g)P_F^2 + \frac{1}{2}(f - \frac{1}{2}g)P_A^2 + \frac{1}{8}h(P_F^4 + 6P_F^2P_A^2 + P_A^4) - EP_F, \quad (4)$$

where the sublattice polarizations P_a and P_b are replaced by the linear combinations

$$P_F = P_a + P_b, \quad P_A = P_a - P_b.$$

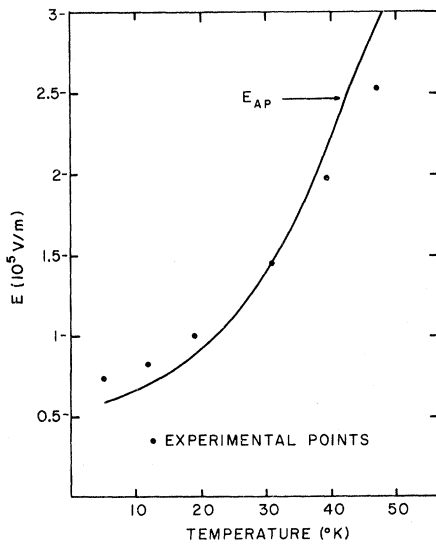


FIG. 4. Field required to induce switching as a function of temperature in an unannealed crystal of SrTiO₃.

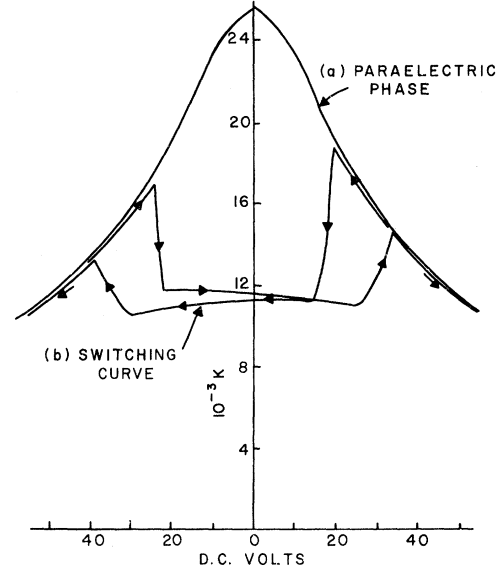


FIG. 5. Electric field dependence of the weak-field dielectric permittivity at 5 °K for an annealed crystal in [100] orientation. Note sample in [100] orientation and 0.43 mm thick: (a) paraelectric phase; (b) antiferroelectric-paraelectric switching.

Conditions for stability are

$$\frac{\partial G}{\partial P_F} = E, \quad \frac{\partial G}{\partial P_A} = 0,$$

$$\text{where } \frac{\partial^2 G}{\partial P_F^2} \frac{\partial^2 G}{\partial P_A^2} - \left(\frac{\partial^2 G}{\partial P_F \partial P_A} \right)^2 > 0. \quad (5)$$

In the paraelectric phase $P_A = 0$, and the energy function reduces to

$$G_F = G_0 + \frac{1}{2}(f + \frac{1}{2}g)P_F^2 + \frac{1}{8}hP_F^4 - EP_F. \quad (6)$$

It is this function that we have used in the analysis of the unannealed crystal dielectric data, and therefore, in the low-field limit

$$\chi_F = f + \frac{1}{2}g = \chi_{100}. \quad (7)$$

Comparing Eqs. (1) and (6), we note that

$$\frac{1}{8}h = B = 0.135 \times 10^{10}. \quad (8)$$

Similarly, in the antiferroelectric state, under low fields, the stability criteria derived from Eq. (4) give

$$P_A^2 = - (2/h)(f - \frac{1}{2}g) \quad (9)$$

$$\text{and } \chi_A = -2(f - g). \quad (10)$$

If we assume as was suggested earlier, that below 62 °K the crystal cooled short circuited is in the antiferroelectric state, then the reciprocal susceptibility measured for this state will be χ_A .

Thus, knowing both χ_F and χ_A over the whole range from 62 to 5 °K, the temperature dependence

of f and g may be determined by combining (7) and (10), giving

$$f = \frac{1}{6}(4\chi_F - \chi_A) \quad \text{and} \quad g = \frac{1}{3}(2\chi_F + \chi_A) \quad (11)$$

At the transition temperature $P_A = 0$, so that from Eq. (9) $f = \frac{1}{2}g$. Below 62 °K the temperature dependence of f , g , and P_A are shown in Figs. 6 and 7.

Using the conditions for stability, equations may be derived for the field dependence of the polarizations P'_F and P_F in the paraelectric and antiferroelectric states, which take the simple forms

$$E_A = \chi_A P_F - 4H P_F^3$$

in the antiferroelectric state, and

$$E_F = \chi_F P'_F + \frac{1}{2}h P'_F{}^3$$

in the paraelectric state. By considering the criterion obtained from the second partial derivatives, two conditions for switching may be derived.

(a) If the E_A curve intersects the E_F curve before E_A reaches a maximum, then the antiferroelectric state disappears at this point of intersection and there is no intrinsic hysteresis between rising and falling fields.

(b) If the E_A curve reaches a maximum before intersecting the E_F curve, the polarization switches discontinuously at this point to the equivalent field point of the E_F curve. On cooling, the state remains polar until the E_F curve intersects the E_A curve when intrinsic instability again appears and

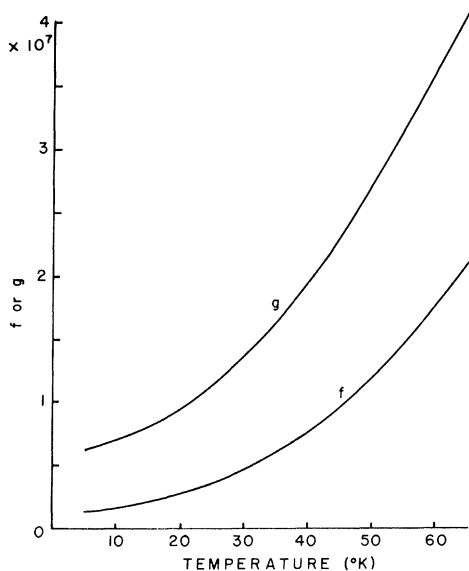


FIG. 6. Temperature dependence of the thermodynamic coefficients f and g deduced from weak-field permittivities.

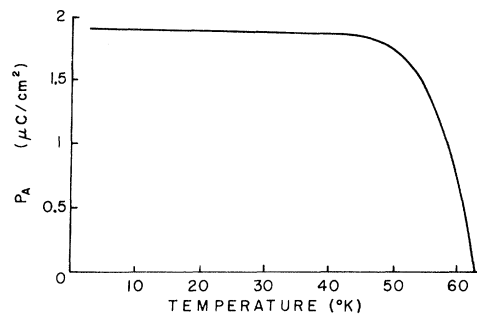


FIG. 7. Antiferroelectric polarization P_A as a function of temperature in an annealed single crystal of SrTiO_3 .

the state reverts to the lower branch of the E_A curve.

Both types of behavior are evidenced for the function used to describe SrTiO_3 , and are shown in Figs. 8–10 which compare observed and predicted behavior at 5, 11.2, and 38 °K.

To summarize this information, in Fig. 4 we compare the fields required to drive the antiferroelectric-paraelectric transition as observed experimentally and as calculated for the whole temperature range.

C. General

It is clear from the above analysis that the Kittel function gives quite surprising agreement with the observed switching in the annealed SrTiO_3 . However, we wish to emphasize that in the above analysis (a) all constants are prescribed by low-field and very high-field measurements, (b) the analysis is strictly valid only for a one-dimensional case, and is here applied to a near cubic crystal, and (c) the effects of any residual mechanical stress have been completely neglected.

In spite of the above, there is good agreement between the calculated and the experimental values of switching fields and polarization as is evident from Figs. 8–10. However, a number of questions still remain. In particular, first, why do unannealed SrTiO_3 crystals show no double loops under any circumstances? Second, what is the function of short circuiting the electrodes in improving the reproducibility of the antiferroelectric phase?

It is not possible at present to make any definite response to these questions; however, we would speculate as follows:

(i) In SrTiO_3 , single crystals, below 60 °K the free energies for paraelectric, ferroelectric, and antiferroelectric states must be closely similar. For example, an estimate of the free-energy difference between paraelectric and antiferroelectric

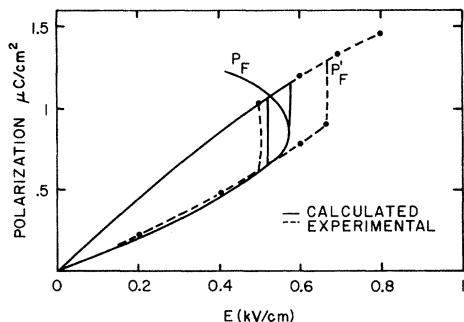


FIG. 8. Calculated and observed dielectric hysteresis at 5 °K.

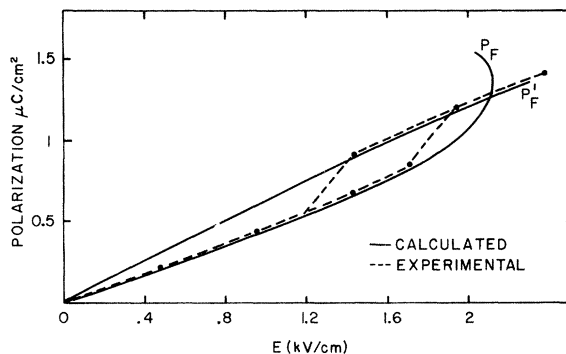


FIG. 10. Calculated and observed dielectric hysteresis at 38 °K.

states can be made from Eq. (4) by substituting $P_F = 0$ and the value of P_A^2 from Eq. (9). This gives $\Delta G = (2h)^{-1}(f - \frac{1}{2}g)^2 \approx 10^{-4} \text{ J/cm}^3$ at 5 °K, which is clearly a very small difference.

(ii) For any given sample, the stable state at low temperature may depend in a critical manner on the boundary conditions of electric field and mechanical stress which existed as the crystal cooled.

(iii) It is possible, indeed likely, that in most crystals there will be a mixture of states depending on local stress and fields.

In unannealed single crystals, we would agree with the tentative conclusion of Sawaguchi⁴ that probably the majority of the crystal is paraelectric with a small admixture in the ferroelectric state. The small ferroelectric fraction would account for (1) the weak dielectric hysteresis first observed by Weaver⁹ at temperatures below 62 °K, (2) the irreversibility between initial and all subsequent dc bias experiments at low temperatures, and (3) the absence of the antiferroelectric state.

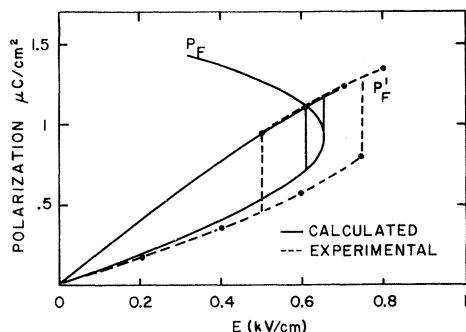


FIG. 9. Calculated and observed dielectric hysteresis at 11.2 °K.

Since the electric field required to eliminate the antiferroelectric state is so small, weak depolarizing fields from ferroelectric regions in the paraelectric matrix would probably suffice to eliminate this phase.

In the annealed crystals, the major effect of annealing has been to reduce internal strain (as evident optically) and thus, probably, also to reduce the ferroelectric fraction. This is evident rather directly in that when cooled open circuited, the annealed crystals show simple S-shaped saturation curves at 50 Hz with no evidence of hysteresis.

If the ferroelectric fraction were completely eliminated, it would be difficult to account for the effects of electrical boundary conditions on stability. Clearly, however, if some very small ferroelectric fraction remains, under open-circuit conditions, to minimize energy the axes of these regions will tend to lie in the plane of the plate and subsequent short circuiting will not eliminate the depoling field which results.

Cooling the crystal short circuited, however, ferroelectric regions will tend to form with axes normal to the plane of the plate, where the depoling field may be eliminated.

Obviously, the explanations offered here are tentative and highly speculative. It must be stressed that annealing is a difficult and, for the crystal, a hazardous operation, and we would stress that it has not been possible to measure a truly representative number of samples. Much more work will be necessary to confirm and extend these measurements. In one sample, however, we have been able to confirm by repeated measurement over a sequence of some 20 low-temperature runs, the differences between open- and short-circuit behavior; and the fact that the double hysteresis phenomenon was not just a "lucky chance" twin pattern but could be achieved repeatedly.

- *Present address: Western Electric Co., Engineering Research Center, P. O. Box 900, Princeton, N. J.
- ¹A. S. Barker, Phys. Rev. 145, 391 (1966).
- ²W. G. Spitzer *et al.*, Phys. Rev. 126, 1710 (1962).
- ³R. A. Cowley, Phys. Rev. 139, A981 (1964).
- ⁴E. Sawaguchi, A. Kikuchi, and Y. Kodera, J. Phys. Soc. Japan 17, 1666 (1962).
- ⁵F. W. Lytle, J. Appl. Phys. 35, 2212 (1964).
- ⁶L. E. Cross and D. Chakravorty, in *Proceedings of the International Meeting on Ferroelectricity* 1, 1966 (Czechoslovakia Academy of Sciences, Prague, 1966), p. 394.
- ⁷W. I. Dobrov, R. F. Vieth, and M. E. Browne, Phys. Rev. 115, 79 (1959).
- ⁸L. Rimai and G. A. DeMars, Phys. Rev. 127, 702 (1962).
- ⁹H. E. Weaver, J. Phys. Chem. Solids 11, 274 (1959).
- ¹⁰E. Hegenbarth, Phys. Status Solidi 6, 333 (1964).
- ¹¹D. Itschner, Ph. D. thesis, Swiss Technical Institute, Zurich (unpublished).
- ¹²P. A. Fleury, J. F. Scott, and J. M. Worlock, Phys. Rev. Letters 21, 16 (1968).
- ¹³G. Shirane and K. Yamada, Phys. Rev. 177, 858 (1969).
- ¹⁴A. E. Paladino, L. G. Rubin, and J. S. Waugh, J. Phys. Chem. Solids 26, 391 (1965).
- ¹⁵A. A. Giardini, J. Opt. Soc. Am. 47, 726 (1957).
- ¹⁶W. H. Rhodes, J. Am. Ceram. Soc. 49, 110 (1966).
- ¹⁷P. A. Fleury and J. M. Worlock, Phys. Rev. 174, 613 (1968).
- ¹⁸L. E. Cross, J. Phys. Soc. Japan 23, 77 (1967).
- ¹⁹K. Okada, J. Phys. Soc. Japan 27, 420 (1969).
- ²⁰A. F. Devonshire, Phil. Mag. 3, 86 (1954).

Classical Heisenberg Magnet in Two Dimensions*

R. E. Watson, M. Blume, and G. H. Vineyard
Brookhaven National Laboratory, Upton, New York 11973
 (Received 20 March 1970)

The equilibrium properties of a square planar array of classical spins with near-neighbor Heisenberg interactions have been examined for arrays of up to 2025 spins with and without periodic boundary conditions. Equilibrium values of the root-mean-square magnetization M_{rms} were obtained by Monte Carlo calculations. Sample spin arrays whose energy agreed with the ensemble average at a given temperature were taken as characteristic of that temperature and were employed to obtain instantaneous correlation functions. The results are less clear than those reported previously for three-dimensional systems: The Monte Carlo calculations converged more slowly because of the lower connectivity of the lattice, and, unlike the three-dimensional case, the short-range order has a range as large, or larger, than the largest sample dimensions. The results are consistent with the observation of Mermin and Wagner that the system does not order ferromagnetically at finite temperatures, and lend some credence to the conjecture of Stanley and Kaplan on the existence of a special ordered state possessing "long-ranged short-range order."

I. INTRODUCTION

In an earlier paper,¹ we have presented results of extensive computer studies of a three-dimensional classical Heisenberg ferromagnet. That paper reported Monte Carlo calculations of the magnetization and the static spin correlations at various temperatures in various sizes of arrays. Also given were the time-displaced spin-correlation functions, found by numerically integrating the classical equations of motion for the entire system of spins. The same computer methods are readily extended to arrays of other dimensionality. The static properties of a two-dimensional array of three-dimensional spins are of interest because of the fact that a ferromagnetic state does not exist in near-neighbor coupled two-dimensional

Heisenberg systems and because of associated questions concerning the existence of a nonferromagnetic state which nevertheless possesses some kind of long-range order.^{2,3} Consequently, we have made Monte Carlo calculations of such two-dimensional systems of a variety of sizes and at a variety of temperatures.

In the next two sections, we review the method of calculation and summarize the results. A fuller discussion of the Monte Carlo procedure is given in I.

II. MODEL AND METHOD OF CALCULATION

Let each site n of a simple square lattice be occupied by a spin \vec{S}_n , where \vec{S}_n is a three-dimensional vector of unit length. Let the energy of the system